Microfluidic labeling of biomolecules with radiometals for use in nuclear medicine

Tobias D. Wheeler,[ab] Dexing Zeng,[c] Amit V. Desai,[ab] Birce Önal,[bc] David E. Reichert[c] and Paul J. A. Kenis*[ab]

Received 1st July 2010, Accepted 10th September 2010
DOI: 10.1039/c0lc00162g

Radiometal-based radiopharmaceuticals, used as imaging and therapeutic agents in nuclear medicine, consist of a radiometal that is bound to a targeting biomolecule (BM) using a bifunctional chelator (BFC). Conventional, macroscale radiolabeling methods use an excess of the BFC–BM conjugate (ligand) to achieve high radiolabeling yields. Subsequently, to achieve maximal specific activity (minimal amount of unlabeled ligand), extensive chromatographic purification is required to remove unlabeled ligand, often resulting in longer synthesis times and loss of imaging sensitivity due to radioactive decay. Here we describe a microreactor that overcomes the above issues through integration of efficient mixing and heating strategies while working with small volumes of concentrated reagents. As a model reaction, we radiolabel 1,4,7,10-tetraazacyclododecane-1,4,7,10-tetraacetic acid (DOTA) conjugated to the peptide *cyclo*(Arg-Gly-Asp-DPhe-Lys) with $^{64}Cu^{2+}$. We show that the microreactor (made from polydimethylsiloxane and glass) can withstand 260 mCi of activity over 720 hours and retains only minimal amounts of $^{64}Cu^{2+}$ (<5%) upon repeated use. A direct comparison between the radiolabeling yields obtained using the microreactor and conventional radiolabeling methods shows that improved mixing and heat transfer in the microreactor leads to higher yields for identical reaction conditions. Most importantly, by using small volumes (~10 μL) of concentrated solutions of reagents (>50 μM), yields of over 90% can be achieved in the microreactor when using a 1 : 1 stoichiometry of radiometal to BFC–BM. These high yields eliminate the need for use of excess amounts of often precious BM and obviate the need for a chromatographic purification process to remove unlabeled ligand. The results reported here demonstrate the potential of microreactor technology to improve the production of patient-tailored doses of radiometal-based radiopharmaceuticals in the clinic.

1 Introduction

Nuclear imaging and therapy are vital to several areas of modern medicine, including oncology, cardiology, hematology, and studies of the biodistribution of drugs.[1,2] These non-invasive techniques rely on the introduction of radioactive agents (radiopharmaceuticals) into the body to detect disease *via* Positron Emission Tomography (PET) or Single Photon Emission Computed Tomography (SPECT), or to treat disease with ionizing radiation. To minimize the systemic exposure of the body to radiation, and to enhance the specificity and sensitivity of the PET and SPECT imaging techniques, metallic radionuclides (radiometals) are bound to biomolecules (BMs) with bifunctional chelators (BFCs).[3] The BM (*e.g.*, a peptide or an antibody) is selected to have a high affinity for the tissue of interest, to deliver and retain radiation only where it is needed. The BFC is selected to have a high affinity for the radiometal, form a complex with the radiometal that is highly stable *in vivo*, and possess a functional group that can form a bond with the biomolecule.

Two radionuclides commonly used in nuclear imaging are the positron emitter ^{18}F (used in PET), and the gamma ray emitter ^{99m}Tc (used in SPECT). These radionuclides have relatively short half-lives (109 minutes and 6 hours, respectively) that make them favorable for minimizing exposure of the body to radiation, and have decay characteristics that make them optimal for their respective imaging modalities. The relatively short half-life of ^{18}F and its typical labeling conditions (use of organic solvents) lowers its suitability for use with biomolecules such as antibodies and peptides. An alternative radionuclide that has received increasing attention is the positron emitter $^{64}Cu^{2+}$.[4–6] The decay properties of this radiometal allow it to be used both as a PET imaging agent[4–7] and as a nuclear therapy agent.[5,6,8] In addition, its half-life of 12.7 hours, and the fact that large quantities with high specific activity (>10 000 mCi mol^{-1}) can be produced at a cyclotron from enriched ^{64}Ni,[3] facilitate the distribution of $^{64}Cu^{2+}$ from a central production facility. Further benefits associated with $^{64}Cu^{2+}$ include: (1) its well-documented coordination chemistry, redox chemistry, and biochemistry and metabolism in humans; (2) the availability of a variety of aza-macrocyclic BFCs that can chelate copper in the 2+ oxidation state with high specificity and stability; and (3) the ability to perform radiolabeling reactions in protein-friendly, aqueous

[a]*Institute for Genomic Biology, University of Illinois at Urbana Champaign, 1206 W. Gregory Dr., Urbana, IL, 61801, USA. E-mail: kenis@illinois.edu*
[b]*Department of Chemical & Biomolecular Engineering, University of Illinois at Urbana Champaign, 600 S. Mathews Ave., Urbana, IL, 61801, USA*
[c]*Radiological Sciences Division, Mallinckrodt Institute of Radiology, Washington University School of Medicine, Campus Box 8225, 510 South Kingshighway, St Louis, MO, 63110, USA*

media (as opposed to the organic solvents required for radiolabeling with ^{18}F), at pH ~7, and at near-physiological temperatures.[9]

Conventional radiolabeling methods for radiometals such as $^{64}Cu^{2+}$ typically require the dilution of small quantities of picomolar radiometal solution for convenient handling and proper mixing, resulting in nanomolar concentrations of the radiometal.[6,10–12] This dilution requires a large excess (~100-fold compared to the radiometal concentration) of the potentially expensive and difficult-to-obtain BFC–BM conjugate to ensure the desired high percentage of bound radionuclide (>90%) within a reasonable time (<1 hour). In turn, the use of large excesses of BFC–BM conjugate necessitates extensive chromatographic purification to remove unlabeled BFC–BMs and to obtain the high specific activities that are desirable for application of the radiopharmaceutical, for example in PET imaging. Chromatographic purification is also potentially required to remove BFC–BM impurities that may bind more strongly or more quickly to the radiometal than the desired BFC–BM conjugate. For instance, if the 100-fold excess of BFC–BM contains 1% impurity, then the molar ratio of impurity to radiometal would be 1 : 1, potentially leading to the synthesis of unwanted radiometal–ligand complexes.

In this report, we demonstrate the utility of microfluidics to overcome some of the drawbacks associated with conventional radiolabeling methods mentioned above. Previous efforts on microfluidic approaches for the synthesis of radiopharmaceuticals focused primarily on the synthesis of ^{18}F- and ^{11}C-labeled agents.[13–15] For example, Lee *et al.*[16] designed an intricate poly(dimethyl siloxane) (PDMS)-based microreactor for the multistep synthesis of ^{18}F-FDG, a radiotracer commonly used to detect cancer *via* PET. An improved version of this microreactor provided yields of 96% after ~15 minutes of total synthesis time, compared to 75% yield after ~45 minutes using an automated apparatus for conventional synthesis.[17] However, an off-chip purification step was still required to give a radiochemical purity of ~99%, and loss of ^{18}F through reaction with or absorption by the PDMS was noted as a significant issue. In other work, Lu *et al.* investigated the effect of infusion rate, *i.e.*, residence time, on the yields of several ^{18}F and ^{11}C-labeled carboxylic esters using a T-junction, flow-through glass microreactor.[18] Of relevance to our work, they observed that incomplete diffusive mixing at lower residence times adversely affected the yield.

Here we report on the design, fabrication, and validation of a PDMS/glass-based microreactor for radiolabeling biomolecules with $^{64}Cu^{2+}$ or other radiometals that exploits several key attributes of microfluidics. (1) The ability to manipulate small volumes of reagents (from μL to pL), which eliminates the need for the dilution of radionuclides, potentially obviating the need to use excess ligand and the associated chromatographic purification steps. (2) The overall small size of the microreactor and peripherals, which reduces space requirements and radioactivity shielding costs. (3) The small volumes of reactants and the small dimensions of the reactor, which sidestep some of the heat and mass transport limitations encountered in macro-scale radiolabeling. Here we also use staggered herringbone grooves[19] to passively mix reagents and thereby further reduce mass transport limitations. We successfully validate the microreactor-based approach by comparison with conventional procedures for radiolabeling using the chelation of $^{64}Cu^{2+}$ by 1,4,7,10-tetraazacyclododecane-1,4,7,10-tetraacetic acid (DOTA) conjugated to the peptide *cyclo*(Arg-Gly-Asp-DPhe-Lys)(*cyclo*(RGDfK)) which is a potential imaging agent in the detection of cancer *via* PET.[7,12,20–22]

2 Design and testing

2.1 Design of the microreactor

We present here a PDMS-based, microfluidic reactor for labeling BFC–BMs with radiometals (Fig. 1). The microreactor consists of three key elements: (1) a serpentine microchannel for mixing, in which we defined staggered herringbone grooves[19] using soft lithography; (2) a series of reservoirs for the incubation of the radiometal–ligand mixture and (3) a thin-film heater for heating the mixture.

2.1.1 Serpentine mixing channel. The microreactor incorporates a passive mixer developed by Stroock *et al.*[19] to minimize diffusive limitations to the overall rate of the radiolabeling reaction. Generally, in the laminar, low Reynolds number flow that occurs at the microscale, when two streams of reagents are brought in contact, a depletion zone forms as a result of the consumption of the reagents at the interface between the two streams. This depletion zone grows in the transverse direction as the streams flow axially along the channel. As a result, the reagents must diffuse across increasingly longer distances in order for the reaction to proceed. The small scale of microfluidic systems renders them less susceptible to the growth of large depletion zones than macro-scale systems (the distance for diffusion, Δr [m], is ultimately limited to half the width of a microchannel, $w/2 \approx 100$ μm). However, the time scale for diffusion across the channel in microfluidic systems $\tau_D = \Delta r^2/D$, where D [m^2 s^{-1}] is the diffusivity of the reagent, can still be significant (on the order of minutes), particularly for large molecules that have low diffusivities in water ($D < 10^{-11}$ m^2 s^{-1}), such as proteins and antibodies, compared to the time scale of the reaction, $\tau_R = 1/kC_0^n$, where k [M^{-n} s^{-1}] is the reaction rate constant, C_0 [M] is the initial concentration of the reagent, and n is the order of the reaction. Thus, depletion zones can impose diffusive mass transport limitations on the rate of a reaction that occurs in a microchannel and should be avoided, particularly for high-throughput reactions with fast kinetics.

We introduce passive mixing of reagents, generated by staggered herringbone grooves,[19] to further reduce, and potentially eliminate entirely, the limitation to reaction kinetics caused by depletion zones. The staggered herringbone grooves in the mixing channel induce chaotic stirring in the cross-section of the flow that stretches and folds the interface between the co-flowing, laminar streams. This stretching and folding reduces the maximum distance, Δr, that the solutes in the initially separate streams must diffuse in order to form a homogeneous mixture[19] and to react, resulting in smaller depletion zones, and thus a reduced potential for diffusive mass transport limitations on the rate of reaction. The maximum diffusive distance for chaotic stirring can be approximated by, $\Delta r = w/2 \exp(-\Delta y/\lambda)$, where w [m] is the width of the microchannel, Δy [m] is the distance traveled along the axis of the microchannel, and λ [m] is a characteristic length determined by the geometry of the trajectories of the chaotic stirring.[19] Based on this equation and the estimated

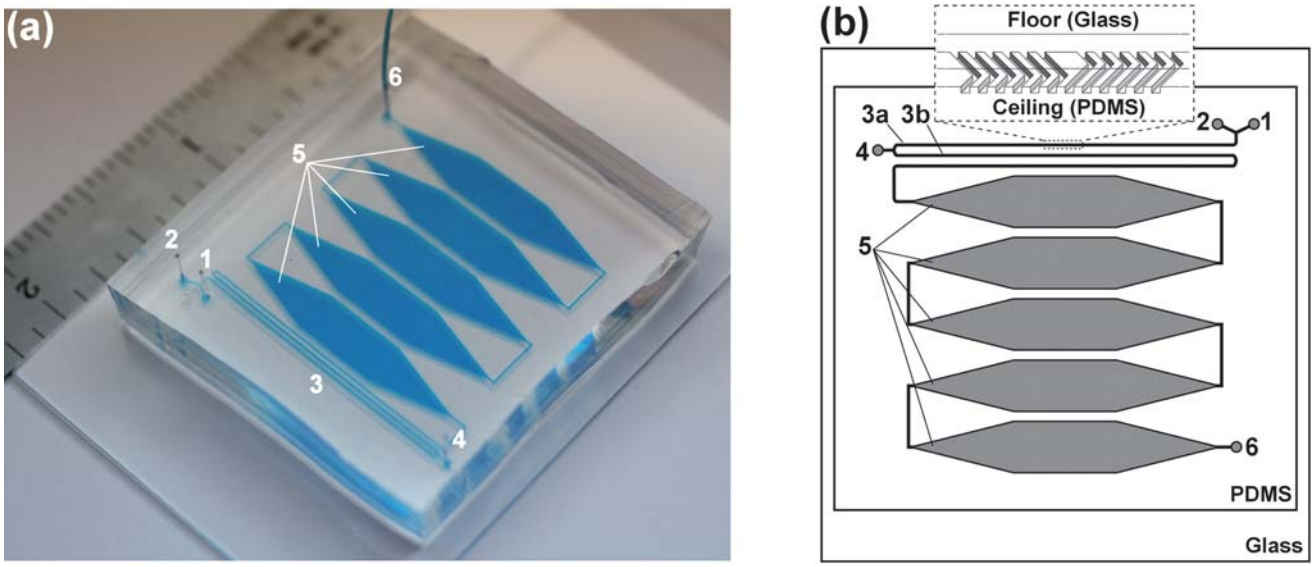

Fig. 1 (a) Photograph and (b) schematic diagram of the microreactor. In (a), the mixing channels and incubation reservoirs are filled with blue dye. In both (a) and (b), 1 is the radiometal inlet, 2 is the buffer inlet, 3 is the serpentine mixing microchannel, 4 is the BFC–BM inlet, 5 are the incubation reservoirs, and 6 is the product outlet. In (b), 3a and 3b are the first and second legs of the mixing channel, respectively. The inset in (b) shows an illustration of the staggered herringbone grooves defined in the PDMS ceiling of the mixing microchannel. The length, width, and height of the PDMS portion of the microreactor are $\sim 2'' \times \sim 1.5'' \times \sim 0.25''$.

value of $\lambda \approx 2$ mm for the chaotic stirring induced by the grooves,[19] once the two streams have reached the end of a 3 cm long, grooved microchannel, Δr will have decreased by roughly six orders of magnitude, yielding a reduction in τ_D of 12 orders of magnitude. This drastic reduction in mixing time eliminates any mass transport limitations to the reaction rates, as is desired for the radiometal labeling chemistries pursued here. Furthermore, the relatively short length of the mixing channel afforded by using chaotic stirring, as opposed to the longer channel lengths that would be required when relying solely on diffusion to mix, enables the use of high flow rates (>500 μL min^{-1}), without developing prohibitively large pressure drops. This aspect will be useful for high-throughput radiolabeling for cases in which chelation rates are fast.

2.1.2 Reservoirs and heater. For the case when chelation rates are slow, the microreactor incorporates a series of reservoirs and a thin film heater. The high degree of homogeneity of the reagent mixture accomplished through the use of the staggered herringbone mixer, allows for the accumulation of clinically relevant volumes of the mixture (up to 50 μL per run) in the reservoirs, without provoking mass transport limitations to the rate of the radiolabeling reaction. If regions of incomplete mixing were present, these regions, and the depletion zones that develop within them, would be magnified through the expansion of the microchannel into the wider reservoir, and diffusive mass transport limitations would be exacerbated. In the microreactor presented here, the well-mixed solution of reagents can be incubated for arbitrary periods of time at elevated temperatures to achieve high yields, and then flushed quickly from the microreactor for use. The microreactor itself can withstand elevated temperatures, however, bubbles form within the microchannels and reservoirs when the system is heated above 65 °C, presumably due to the expansion of microscopic pockets of air and water vapor trapped between the liquid and wall. Degassing the reagents suppresses the formation of these bubbles.

The simple features discussed above combine to allow the microreactor to perform both high-throughput, continuous flow radiolabeling for fast chelation rates, and semi-batch, incubated radiolabeling for slow chelation rates. In addition, the simplicity of the design (*i.e.*, the lack of extensive networks of microchannels and of valves and their required ancillary equipment) is beneficial for its envisioned use in the clinic as an inexpensive, disposable microreactor for the custom, on-demand synthesis of radiopharmaceuticals.

2.2 Testing of the microreactor

We validated the microreactor by labeling a BFC–BM conjugate with $^{64}Cu^{2+}$. The BFC–BM conjugate consisted of the bifunctional chelator 1,4,7,10-tetraazacyclododecane-1,4,7,10-tetraacetic acid (DOTA), and the peptide *cyclo*(Arg-Gly-Asp-DPhe-Lys) (*cyclo*(RGDfK)). This peptide targets $\alpha_V\beta_3$ integrin, a receptor that is up-regulated on the surface of cells undergoing angiogenesis.[20] The high occurrence of angiogenesis in tumors results in a higher concentration of $\alpha_V\beta_3$ integrin, and therefore a higher concentration of bound, radiolabeled RGD, in contrast with the surrounding, healthy tissue. Radiolabeled RGD-based imaging agents are promising candidates for the imaging of tumors *via* PET.[7,12,20–22]

The radiolabeling method, summarized in Scheme 1, consists of three steps: (1) the addition of $^{64}Cu^{2+}$ in 0.1 N HCl (the state of the radiometal as it is received the cyclotron) to 10 mM ammonium acetate (NH_4OAc) (pH = 6.8) to form $^{64}Cu(OAc)_2$ through ligand exchange; (2) the addition of DOTA-*cyclo*(RGDfK) in 10 mM NH_4OAc (pH = 6.8) to the $^{64}Cu(OAc)_2$ mixture to form ^{64}Cu-DOTA-*cyclo*(RGDfK) through chelation; (3) the incubation of the ^{64}Cu-DOTA-*cyclo*(RGDfK) mixture at room or

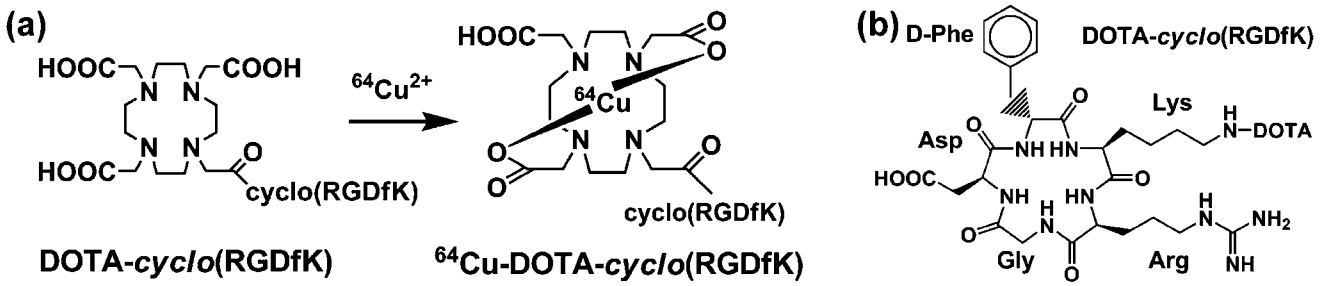

Scheme 1 Chelation of $^{64}Cu^{2+}$ by DOTA-*cyclo*(RGDfK). (a) The reaction scheme of the chelation of $^{64}Cu^{2+}$ by DOTA-*cyclo*(RGDfK). Of the four pendant arms of DOTA, two are used in chelation of the radiometal and one is used to conjugate the biomolecule *cyclo*(RGDfK). (b) The structure of *cyclo*(RGDfK) and the position at which DOTA is conjugated to the biomolecule.

elevated temperature to drive the chelation reaction to completion. The two-step combination of reagents is performed in the serpentine mixing channel of the microreactor, with radiometal and buffer solutions mixing in the first leg of the channel (3a in Fig. 1b) and ligand and radiometal-buffer solutions mixing in the second leg of the channel (3b in Fig. 1b).

After passing through the mixing channels, the reagents flow into the reservoirs, where they are incubated at room or elevated temperatures for a certain period of time. This incubation step is necessary, as the chelation of $^{64}Cu^{2+}$ by DOTA-*cyclo*(RGDfK) likely involves the rate-limiting rearrangement of a di- or monoprotonated intermediate before chelation is complete, as is the case for the formation of lanthanide complexes (Ln^{3+}) with DOTA–peptide conjugates.[23]

3 Materials and methods

3.1 Chemicals

RTV 615 poly(dimethyl siloxane) (PDMS) was obtained from General Electric Company (Waterford, NY). SU-8 2050 was obtained from MicroChem Corporation (Newton, MA). (Tridecafluoro-1,1,2,2-tetrahydrooctyl)trichlorosilane was obtained from Gelest, Inc. (Morrisville, PA). *Cyclo*(RGDfK) was purchased from Peptides International, Inc. (Louisville, KY). 1,4,7,10-Tetraazacyclododecane-1,4,7,10-tetraacetic acid mono(*N*-hydroxysuccinimide ester)(DOTA-NHS-ester) was purchased from Macrocyclics (Dallas, TX). $^{64}Cu^{2+}$ in 0.1 M HCl was produced at Washington University School of Medicine, and obtained through the Radionuclide Resource for Cancer Applications. De-ionized water (DI-H_2O) was produced using a Millipore Milli-Q water system. All other chemicals and solvents were purchased from Sigma-Aldrich (St Louis, MO).

3.2 Equipment

Three sets of female 1/4–28 to female Luer lock adaptors with ferrules and nuts, PEEK tubing of 1/16″ OD and 0.01″ ID, and a NanoTight kit with 1/16″ × 0.027″ FEP sleeves, obtained from Upchurch Scientific (Oak Harbor, WA) and Microbore PTFE tubing (0.012″ ID × 0.030″ OD) obtained from Cole-Parmer (Vernon Hills, IL) were assembled to connect syringes to the microreactor. The 75 mm × 50 mm × 1 mm glass slide, used to assemble the microreactor, and the Fisher Vortex Genie 2 were obtained from Fisher Scientific (Pittsburgh, PA). A test grade, 3″ silicon wafer, obtained from University Wafer (South Boston, MA) was used to fabricate the SU-8 mold for the microreactor. Three microlitre flow modular pump components, which included a syringe pump, a pump driver circuit, and a power supply, were obtained from Harvard Apparatus (Holliston, MA). The Kapton-insulated, 2″ × 2″, thin film heater, the Omega CN740 temperature controller, and an Omega SA 1-RTD probe were obtained from Omega Engineering (Stamford, CT). The Harrick plasma cleaner was obtained from Harrick Plasma (Ithaca, NY). Eppendorf tubes were obtained from MIDSCI, Inc. (St Louis, MO). The BioScan AR-2000 radio-TLC plate reader was purchased from Bioscan, Inc. (Washington, DC). The Thermomixer was obtained from Eppendorf North America (Hauppauge, NY). Radio-TLC plates were obtained from Whatman Thin Layer Chromatography (Piscataway, NJ). Gas-tight, microlitre syringes were obtained from Hamilton Co. (Reno, NV). The 2695 Waters HPLC system used in the purification of DOTA-*cyclo*(RGDfK) was obtained from Waters Corporation (Milford, MA). The Capintec CRC-712M radioisotope dose calibrator used to measure activities for retention experiments was obtained from Capintec, Inc. (Ramsey, NJ). The MS data obtained *via* LC-MS were collected with a Micromass ZQ4000 from Waters Corporation (Milford, MA).

3.3 Synthesis and purification of DOTA-*cyclo*(RGDfK)

DOTA-*cyclo*(RGDfK) was prepared by reacting a solution of 6.03 mg *cyclo*(RGDfK) and 14.0 μL triethylamine (10 eq.) in 1.0 mL dimethylformamide (DMF) with 8.38 mg DOTA-NHS (1.1 eq.). After stirring for 3 hours at room temperature, 3 mL of DI-H_2O were added and stirred for another 30 minutes to hydrolyze the excess DOTA-NHS ester. The crude DOTA-*cyclo*(RGDfK) was then purified on a Waters HPLC system using an Alltech Econosil C18 semi-preparative column (10 μm, 4.6 mm × 250 mm) with a mobile phase of 15 vol% acetonitrile and 85 vol% de-ionized water with 0.1 vol% trifluoroacetic acid (TFA), at a flow rate of 3.0 mL minute^{-1}. Under these conditions, the DOTA-*cyclo*(RGDfK) eluted at 13.5 minutes. The identity and purity of the purified DOTA-*cyclo*(RGDfK) peptide was confirmed by LC-MS using an Phenomenex Luna C18(2) column (5 μm, 100 Å, 4.6 mm × 150mm). The analysis was performed using the following gradient of 0.1 vol% TFA in de-ionized water (A) and 0.1 vol% TFA in acetonitrile (B) with a flow rate of 1.0 mL minute^{-1}: 0–3 minutes: 90% A, 10% B; 13 minutes: 85% A, 15% B; 20–24.5 minutes: 50% A, 50% B; 25–30 minutes: 90% A, 10% B. A UV chromatogram and a TIC

chromatogram are shown in Fig. 2a and b, respectively. The mass spectrum of the peak at ~12 minutes is shown in Fig. 2c, and demonstrates that the peak corresponds to pure DOTA-*cyclo*(RGDfK), with $M^{1+} = 990.9$ and $M^{2+} = 496.4$.

3.4 Fabrication of the microreactor

The microreactor was fabricated using SU-8-based soft-lithography techniques for PDMS.[24] The dimensions of the features shown in Fig. 1 are as follows: serpentine microchannel (100 μm high, 200 μm wide, 10.7 cm long), five hexagonal reservoirs (100 μm high, 5 mm wide, 3 cm long), microchannels between reservoirs (100 μm high, 200 μm wide, 7.2 mm long). The staggered herringbone grooves in the mixing channels (see expanded view in Fig. 1b) were designed to have the same geometry as those developed by Stroock *et al.*[19] An SU-8 mold of the features was fabricated as follows: (1) negative images of the microchannels, inlets, outlets, and reservoirs were printed on one transparency film and those of the grooves were printed on a second transparency film, using a 5080 dpi printer; (2) the pattern of the microchannels, inlets, outlets, and reservoirs was transferred from the first transparency to a 100 μm thick layer of SU-8 2050 spun onto a silicon wafer, *via* photolithography; (3) the pattern of the grooves was transferred from the second transparency to a second, 50 μm thick layer of SU-8 2050 that was spun over the first layer, following an alignment step so as to define the grooves directly above the mixing channel; (4) unexposed SU-8 was dissolved using propylene glycol methyl ether acetate (PGMEA), and the exposed silicon surface was passivated *via* vapor deposition of (tridecafluoro-1,1,2,2-tetrahydrooctyl) trichlorosilane, under vacuum. PDMS (10 : 1 ratio of precursor to curing agent) was then poured over the SU-8 mold and cured at 60 °C for 2+ hours. The cured PDMS was removed from the mold, inlet and outlet holes were punched, and the PDMS was bonded to a 75 mm × 50 mm × 1 mm glass slide, after 1 minute plasma treatment of both components with a Harrick Plasma Cleaner (RF level: Hi, Pressure: 500–1000 mTorr), followed by baking at 60 °C for 12 hours.

3.5 Operation of the microreactor

The microreactor was operated in semi-batch mode. Upon entering the microreactor through inlets 1 and 2, respectively, a radiometal solution and a buffer solution flowed through the mixing channel (3 in Fig. 1). As the two solutions flowed along the microchannel, they were mixed by the chaotic advection induced by the geometry of the grooves.[19] Once the buffer and radiometal solutions reached the end of the first mixing channel, the ligand (BFC–BM) solution was pumped into the microreactor through inlet 4 and mixed with the radiometal–buffer mixture in a second mixing microchannel with staggered herringbone grooves defined in the ceiling. The mixed reagents then filled a series of five hexagonal reservoirs (5 in Fig. 1), after which the flow was stopped and the mixture was heated to the desired temperature and allowed to react for a specified incubation time. After this incubation time, buffer solution was pumped into the microreactor to flush out the product, through the outlet (6 in Fig. 1), for collection. A schematic diagram of the system used to operate the microreactor is shown in Fig. 3. The flow of each reagent stream, radiometal, buffer, and ligand, into the microreactor was driven by syringe pumps that were controlled by a LabVIEW virtual instrument (VI). Communication between the VI and the syringe pump drivers was facilitated by a serial connection. The VI was used to set the individual flow rates and regulate the timing of the pumps, with inputs for controlling the incubation time, the total flow rate, the desired volume of product (the maximum being the total volume of the reservoirs, ~50 μL), and the stoichiometric molar ratios of buffer-to-radiometal and ligand-to-radiometal. For radiolabeling at elevated temperatures, a thin-film heater, placed in

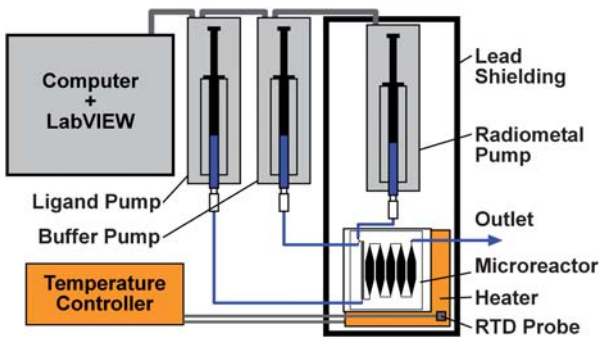

Fig. 3 Schematic diagram of the radiolabeling system. Three LabVIEW-controlled syringe pumps drive the flow of the BFC–BM (ligand), buffer, radiometal solutions into the microreactor. A thin-film heater, controlled using a temperature controller and a resistance temperature detector (RTD) probe affixed to the heater, sets the incubation temperature. Lead shielding surround the microreactor and radiometal pump when operating with radioactive reagents.

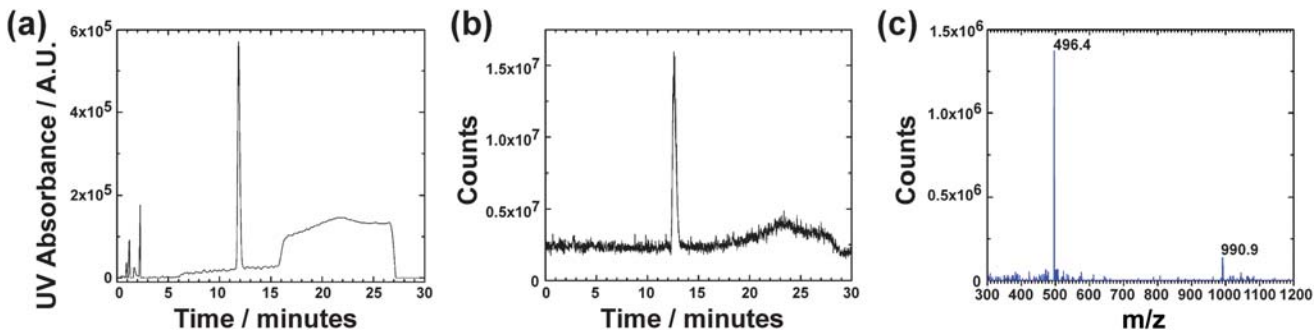

Fig. 2 Purity of DOTA-*cyclo*(RGDfK), as indicated by (a) UV and (b) total ion current (TIC) chromatograms. The mass spectrum of the material corresponding to the peak with an elution time of 12.6 minutes in (b) is shown in (c).

contact with the glass surface of the microreactor, was used to heat the microreactor, and a temperature controller and resistance temperature detector (RTD) probe were used to maintain the temperature within ±1 °C of the desired temperature set-point. The radiometal syringe pump, heater, and microreactor were shielded on four sides and below with 2″ of lead shielding. The radiometal syringe was fitted with a 7.5 cm length of PEEK tubing connected to an Upchurch Luer lock fitting. The PDMS microreactor was fit with a 10 cm length of PTFE tubing connected to an Upchurch NanoTite fitting. The syringe and PEEK "needle" were inserted into the fitting and tightened.

3.6 Measurement of the retention of $^{64}Cu^{2+}$

A 3 cm long, 200 μm wide, 100 μm tall microchannel with staggered herringbone grooves, fabricated from PDMS and glass and with a volume of ~0.6 μL, was used for these experiments. Prior to use, the microchannel was cleaned with 50 μL of 1 N nitric acid to remove trace metals, and flushed with 5 mL of 10 mM NH_4OAc buffer solution.

3.6.1 Pre-treatment with Cu^{2+}/Na^+. 50 μL of a 10 mM $CuCl_2$/NaCl solution were injected into the microchannel and allowed to sit for 30 minutes. The microchannel was then flushed with 5 mL of 10 mM NH_4OAc buffer solution (pH = 6.8).

3.6.2 Retention measurement. 30 μL of no carrier-added (only radioactive) $^{64}Cu^{2+}$ in 10 mM NH_4OAc buffer solution (pH = 6.80) were injected into the microchannel. After 10 minutes, the $^{64}Cu^{2+}$ solution was displaced from the microchannel by 200 μL of air, *via* syringe. The microchannel was then flushed with 200 μL of 10 mM NH_4OAc buffer. The percent of injected activity retained in the microchannel was calculated from the known activity of the injected solution, and the difference between the activity left behind in the microchannel after flushing and the initial activity of the microchannel measured before the $^{64}Cu^{2+}$ solution was injected, all measured with the Capintec radioisotope dose calibrator.

3.7 Radiolabeling of DOTA-*cyclo*(RGDfK)

Stock solutions of carrier-added $^{64}Cu^{2+}$ were prepared by first diluting the solution obtained from the cyclotron (20 mCi $^{64}Cu^{2+}$ in 0.1 M HCl) with 10 mM NH_4OAc (pH = 6.8) to give a specific activity of 1 mCi μL^{-1}. The various copper solutions were then prepared from this original stock solution. In order to prepare a 200 μM carrier-added $^{64}Cu^{2+}$ solution, 20 μL of the 1 mCi μL^{-1} $^{64}Cu^{2+}$ solution were mixed with 20 μL of 10 mM non-radioactive copper solution and 960 μL of 10 mM NH_4OAc (pH = 6.8). The different concentrations of carrier-added $^{64}Cu^{2+}$ solutions listed in Sections 3.7.1 and 3.7.2 were obtained by the dilution of the above 200 μM carrier-added $^{64}Cu^{2+}$ solution with 10 mM NH_4OAc.

Stock solutions of 10 mM DOTA-*cyclo*(RGDfK) were prepared by first dissolving 10.0 mg of purified DOTA-*cyclo*(RGDfK) (Section 3.3) in 100 μL of a mixture of 10 mM NH_4OAc (pH = 6.8) and acetonitrile (MeCN) (50 : 50 vol%), and then diluting these solutions with 10 mM NH_4OAc (pH = 6.8) to give final concentrations of 200, 100, 40, and 2 μM DOTA-*cyclo*(RGDfK).

3.7.1 Conventional radiolabeling procedures. Conventional radiolabeling was performed using two methods: (1) mixing, incubation and heating of a total volume of 10.5 μL of solution with a Thermomixer, and (2) mixing of a total volume of 105 μL of solution using a vortexer, followed by continued mixing, incubation and heating with a Thermomixer. For method (1), 3.0 μL of 100 μM DOTA-*cyclo*(RGDfK) solution were first added to 1.5 μL of 10 mM NH_4OAc (pH = 6.8) in a 1.6 mL Eppendorf tube. Then, 6.0 μL of 50 μM $^{64}Cu^{2+}$ solution were added to the mixture, and the Eppendorf tube was placed in the Thermomixer and incubated for 12 minutes at a temperature of 23, 37 or 47 °C. For method (2), 30 μL of 100 μM DOTA-*cyclo*(RGDfK) solution were first added to 15 μL of 10 mM NH_4OAc (pH = 6.8) in a 1.6 mL Eppendorf tube. Then, 60 μL of 50 μM $^{64}Cu^{2+}$ solution were added to the mixture, the mixture was vortexed for 10 seconds, and the Eppendorf tube was placed in the Thermomixer and incubated for 12 minutes at a temperature of 23, 37 or 47 °C. The final concentration of $^{64}Cu^{2+}$ and DOTA-*cyclo*(RGDfK) was 28.6 μM in both methods. Following the incubation period, the extent of reaction was determined as described in Section 3.7.3.

3.7.2 Microreactor radiolabeling procedure. The general mode of operation of the microreactor is described in Section 3.5. For the radiolabeling experiments summarized in Fig. 6a (effect of residence time on extent of reaction) and Fig. 6b (effect of mixing method and temperature on extent of reaction), the following solutions were used: (1) 50 μM carrier-added $^{64}Cu^{2+}$ solution, (2) 100 μM DOTA-*cyclo*(RGDfK) stock solution, and (3) 10 mM NH_4OAc (pH = 6.8) buffer. Using the LabVIEW interface, the pumps were programmed to combine the radiometal (1), ligand (2), and buffer (3) solutions with the same volumetric ratios as those used for the conventional radiolabeling procedure, giving a ligand-to-metal molar ratio of 1 : 1 and a final concentration of $^{64}Cu^{2+}$ and DOTA-*cyclo*(RGDfK) of 28.6 μM. The total flow rate was set to 50 μL $minute^{-1}$, the total volume was set to 20 μL (an additional 30 μL of buffer was pumped into the microreactor to fill all the reservoirs). For the experiments in Fig. 6a, the temperature was set to 37 °C, and the incubation time was set to 5, 10, and 20 minutes (resulting in total residence times, t_{RES} = 7, 12, and 22 minutes: *e.g.*, 1 minute for filling + 10 minutes for incubation + 1 minute for flushing). For the experiments in Fig. 6b, the incubation time was set to 10 minutes (t_{RES} = 12 minutes), and the temperature was set to 23, 37 and 47 °C. After the collection of product, the extent of reaction was determined as described in Section 3.7.3.

For the radiolabeling experiments summarized in Fig. 7 (effect of concentration on extent of reaction), combinations of stock solutions and buffer-to-metal molar ratio inputs were used to give the following final concentrations of radiometal and ligand (1 : 1 molar ratio): 1 μM (2 μM stock solutions, 1 : 1 buffer-to-radiometal ratio), 10 μM (40 μM stock solutions, 500 : 1 buffer-to-radiometal ratio), 20 μM (40 μM stock solutions, 1 : 1 buffer-to-radiometal ratio), 30 μM (100 μM stock solutions, 130 : 1 buffer-to-radiometal ratio), 50 μM (100 μM stock solutions, 1 : 1 buffer-to-radiometal ratio), and 90 μM (200 μM stock

solutions, 11 : 1 buffer-to-radiometal ratio). Experiments were performed with the same settings as listed above, and with t_{RES} = 12 minutes and at a temperature of 37 °C. After the collection of product, the extent of reaction was determined as described in Section 3.7.3.

Throughout the course of radiolabeling experiments, three trial runs were performed before data were recorded to ensure proper functioning of the microreactor after syringe pump or heater settings were changed and after depleted syringes were replenished.

3.7.3 Measurement of radiolabeling yield. At the end of each reaction run, a 1 μL aliquot of product was spotted onto a radio-TLC plate and developed using a mobile phase of methanol/10% ammonium formate buffer (2 : 1 volume ratio). After developing, the radio-TLC plates were then counted using the Bioscan radio-TLC scanner to quantify free and bound $^{64}Cu^{2+}$. The radiolabeling yields were calculated by dividing the area of the radioactivity peak obtained for the bound $^{64}Cu^{2+}$ by the total area of the radioactivity peaks obtained for both bound and free $^{64}Cu^{2+}$.

4 Results and discussion

4.1 Compatibility of PDMS/glass with $^{64}Cu^{2+}$

We performed the experiments discussed in this section to determine the compatibility of $^{64}Cu^{2+}$with the materials comprising the microreactor. For microfluidic radiolabeling with ^{18}F, the absorption of the radionuclide by PDMS is a significant problem;[14,16,17] up to 95% of an amount of injected activity can be retained.[17] To determine whether similar issues will affect radiolabeling in the current microreactor, we examined the retention of $^{64}Cu^{2+}$ and the ability of PDMS and glass to withstand the emissions of this radionuclide.

In Fig. 4, we plot the percent of injected activity of $^{64}Cu^{2+}$ retained in a single microchannel (length ≈ 3 cm, volume ≈ 0.6 μL) with staggered herringbone grooves defined in the ceiling, for a series of injections of activity. The white bars represent data for a microchannel that has been washed with nitric acid, and the grey bars represent data for a microchannel that has been washed with nitric acid and then pre-treated with a non-radioactive Cu^{2+} solution (Section 3.6). The microchannel that was not pre-treated with Cu^{2+} solution retained a substantial portion of the activity of the first injection (~70%), but retained only ~5% of the activity of subsequent injections. The microchannel that was pre-treated with Cu^{2+} solution retained only ~15% of the activity of the first injection and also retained only ~5% of the activity of subsequent injections. The difference between the retention of the activity in the first injection in the pre-treated and non-pre-treated microchannels, and the decrease in retention of activity in subsequent injections suggest that $^{64}Cu^{2+}$ adheres to the walls of the microchannel, though once the surface is saturated, no further adhesion occurs. The adhesion of the $^{64}Cu^{2+}$ is presumably due to non-specific, electrostatic interactions between the positively charged copper ions and the negatively charged glass surface; polymer coatings with similar chemical groups to those of PDMS are used to minimize electrostatic interactions between positively charged solutes and the surfaces of capillary electrophoresis equipment made of glass.[25]

To confirm the hypothesis that non-specific electrostatic interactions between the microchannel surface and the $^{64}Cu^{2+}$ are

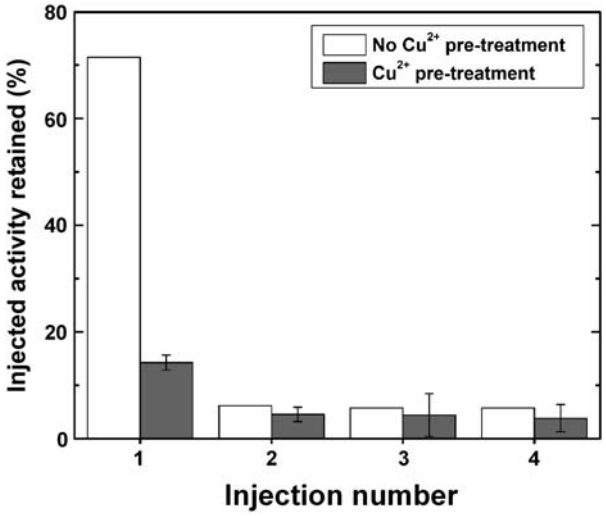

Fig. 4 Retention of $^{64}Cu^{2+}$ in a PDMS/glass microchannel with staggered herringbone grooves. The retention measured without blocking the surface of the microchannel using non-radioactive Cu^{2+} (white bars) is compared to the retention measured after blocking the surface of the microchannel using non-radioactive Cu^{2+} (grey bars). Error bars represent the standard deviations of the averages of multiple experiments (n = 1 for no Cu^{2+} pre-treatment, n = 2 for Cu^{2+} pre-treatment).

responsible for the retention observed in Fig. 4, we used a Na^+ solution to block the surface of the microchannel. Following this pre-treatment, we observed the same decrease in the percentage of injected activity retained as for the case when we pre-treated the microchannel with the Cu^{2+} solution (data not shown). From this and the preceding results, we conclude that the retention of $^{64}Cu^{2+}$ on the glass surface is primarily due to electrostatic interactions and not due to absorption of the ions into the PDMS. The retention of $^{64}Cu^{2+}$ in the microchannel can be minimized either by changing the charge of the glass surface of the microchannel to positive, by functionalizing the glass with a positively charged silane, for example,[25] or by fabricating the microreactor completely in PDMS. Note: in the radiolabeling experiments discussed in later sections, we ignore data for the first three reactions performed in the microreactor. This procedure ensures that the influence of $^{64}Cu^{2+}$ retention on the measured extent of reaction is minimal, by saturating the surface of the microreactor with copper ions.

Over the course of the experiments performed in this work, we used a single microreactor. In total, the device was exposed to 260 mCi of radiation over 720 hours. Only after this exposure did we observe signs of damage—the microreactor began leaking, indicating that the seal between the PDMS and glass had decayed. This leaking was the only instance of mechanical failure that we observed, and occurred after the completion of all experiments reported here (after approximately six months of use). Thus, the device is sufficiently robust for its envisioned role as a single- or multiple-use (<20), disposable microreactor for radiolabeling.

4.2 Microfluidic radiolabeling

In this section, we examine the radiolabeling of DOTA-*cyclo*(RGDfK) with $^{64}Cu^{2+}$ using a 1 : 1 stoichiometric ratio of the two reagents. For the purpose of evaluating the performance

of the microreactor, all experiments were performed using carrier-added $^{64}Cu^{2+}$, so that the concentration of Cu^{2+} was known, and to maximize the number of experiments that could be performed with one batch of the radiometal. Thus, although we refer to $^{64}Cu^{2+}$solutions, over 99% of the copper present in the solutions is not radioactive. The chemical equivalence of radioactive and non-radioactive Cu-DOTA-*cyclo*(RGDfK) is demonstrated by the identical chromatographic elution times of the two molecules (see Fig. 5). For the purpose of operating the microreactor in the clinic, in the production of PET imaging agents, for example, undiluted radiometal solution obtained directly from the cyclotron would be used instead.

In Fig. 6a, we plot the radiolabeling yield (*i.e.*, the percent of $^{64}Cu^{2+}$ chelated by DOTA-*cyclo*(RGDfK)) obtained by mixing 50 μM solutions of $^{64}Cu^{2+}$ and DOTA-*cyclo*(RGDfK) at a 1 : 1 stoichiometric ratio, and incubating the mixture at 37 °C for residence times, t_{RES}, of 7, 12 and 22 minutes. The data indicate that, at this concentration of reagents, over 80% of the radiometal is chelated after 12 minutes. To test reproducibility, the radiolabeling yield for this residence time was measured for solutions made from three separate productions of $^{64}Cu^{2+}$. The standard deviation for this average is larger than those for experiments that were performed with the same batch of $^{64}Cu^{2+}$ (7 and 22 minutes), indicating the variability of the specific activity of the $^{64}Cu^{2+}$ between productions. This variability results in changing amounts of trace metal contaminants that can compete with Cu^{2+} for chelation with DOTA (*e.g.*, Ni, Fe, and Zn).

To contextualize the improvement in radiolabeling provided by the microreactor, we make a direct comparison between the radiolabeling yield obtained by the microreactor and those obtained through conventional radiolabeling methods, again using a 1 : 1 stoichiometric ratio of $^{64}Cu^{2+}$ to DOTA-*cyclo* (RGDfK). To make this comparison, we chose a residence time of 12 minutes and a radiometal/ligand concentration of ~30 μM, such that the radiolabeling yield is high enough to be measured accurately, but does not reach 100% in the microreactor, based on the results in Fig. 6a. Fig. 6b shows the radiolabeling yield for the chelation of $^{64}Cu^{2+}$ by DOTA-*cyclo*(RGDfK) obtained using three different radiolabeling methods at three different temperatures. 'Conventional, 10 μL' and 'Conventional, 100 μL' represent data obtained when the reaction was performed using conventional radiolabeling procedures with small volumes (~10 μL) and large volumes (~100 μL), respectively (Section 3.7.1). The yields obtained using the microreactor at 37 and 47 °C were significantly higher than those obtained using the 10 μL conventional procedure. We speculate that the superior mixing of small volumes of reagents achieved by the microreactor resulted in this improved performance. To support this hypothesis, we compared the yields obtained using the microreactor to those obtained using conventional procedures with a larger volume (Conventional, 100 μL), in which more efficient mixing is possible through vortexing. For both methods, the yield is the same at 23 and 47 °C, within experimental error, indicating that the mixing achieved by the microreactor and by macro-scale vortexing is sufficient to overcome the diffusive mass transfer limitations to the radiolabeling reaction that hinder the performance of the 'Conventional, 10 μL' method. For the microreactor, the yield obtained at 37 °C is the same as that obtained at 47 °C, within experimental error. This result suggests that the microreactor achieves the maximum yield possible for reagent concentrations of ~30 μM and t_{RES} = 12 minutes at a lower temperature than the conventional method, and may also suggest improved performance through enhanced heat transfer in the microreactor.

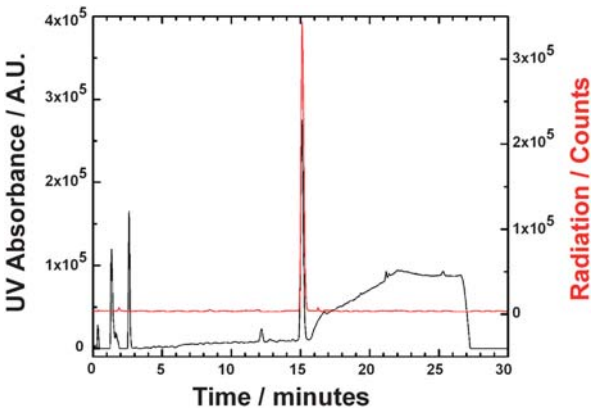

Fig. 5 UV and radio chromatograms for carrier-added ^{64}Cu-DOTA-*cyclo*(RGDfK). Chromatograms of a 50 μM sample synthesized using the conventional method, at T = 37 °C and t_{RES} = 12 minutes (see Section 3.7.1), were obtained using the LC-MS method described in Section 3.3.

In addition to enhancing reaction rates through efficient mass and heat transfer, the ability of microfluidic systems to manipulate small volumes of concentrated reagents can potentially lead to high radiolabeling yields. In Fig. 7, we plot radiolabeling yield as a function of the final concentration of $^{64}Cu^{2+}$, M_F, (*i.e.*, the concentration after all solutions are mixed together) for a stoichiometric ratio of $^{64}Cu^{2+}$ to DOTA-*cyclo*(RGDfK) of 1 : 1, t_{RES} = 12 minutes, and an incubation temperature of 37 °C. The data show that, by increasing the final concentration of the reagents to >50 μM, yields approaching >90% are obtainable with these reaction conditions. Due to the 1 : 1 stoichiometric ratio, the need for the separation of unlabeled BFC–BMs is eliminated once yields reach >90%. The concentration of radiometal obtained from the cyclotron is typically 1–2 mCi ≈ 4 picomoles in ~10 μL, or ~0.4 μM. Final concentrations ≥50 μM could be obtained for the clinical production of radiopharmaceuticals by (1) minimizing the dilution of the radiometal solution by using highly concentrated solutions of buffer and ligand, and (2) implementing a microfluidic means of increasing the concentration of the radiometal, such as through the evaporation of water from the radiometal solution.

5 Conclusions

We present a simple, inexpensive microreactor made from PDMS and glass for radiolabeling biomolecule-bifunctional chelator conjugates (BFC–BMs) with radiometals for application as imaging or therapeutic agents in nuclear medicine. The microreactor is able to efficiently mix small volumes of reagents (~10 μL or less) by using chaotic advection that is induced by staggered herringbone grooves[19] defined in a mixing microchannel in which reagents are combined, and to incubate the reaction mixture at elevated temperatures after it fills several micro-reservoirs (total volume = 50 μL). We tested the

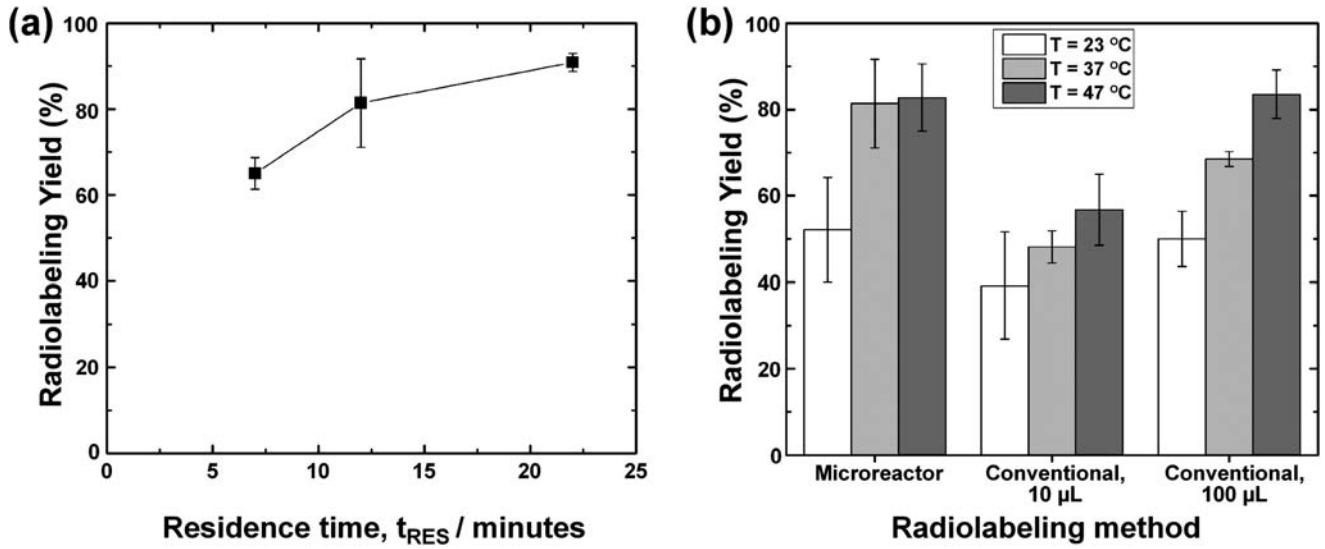

Fig. 6 Radiolabeling yield for the production of ^{64}Cu-DOTA-*cyclo*(RGDfK) as a function of (a) residence time, t_{RES}, and (b) radiolabeling method at various temperatures, T. In (a), error bars represent standard deviation in the extent of reaction for experiments using radiometal solutions made from the same batch of $^{64}Cu^{2+}$ for $t_{RES} = 7$ and 22 minutes ($n = 3$) and between experiments using radiometal solutions made from three different batches of $^{64}Cu^{2+}$ for $t_{RES} = 12$ minutes (3 repetitions for each batch, $n = 9$). Experiments were performed at $T = 37$ °C. Lines between points are guides for the eye. In (b), for the 'Microreactor' method, error bars represent the standard deviation in extent of reaction between three experiments using radiometal solutions made from two ($T = 23$ and 47 °C, $n = 6$) and three ($T = 37$ °C, $n = 9$) different batches of $^{64}Cu^{2+}$. For the other two methods, error bars represent the standard deviation in extent of reaction between three experiments using radiometal solutions made from the same batch of $^{64}Cu^{2+}$ ($n = 3$). Experiments were performed with $t_{RES} = 12$ minutes. All experiments were performed using a 1 : 1 stoichiometric ratio of $^{64}Cu^{2+}$ to DOTA-*cyclo*(RGDfK).

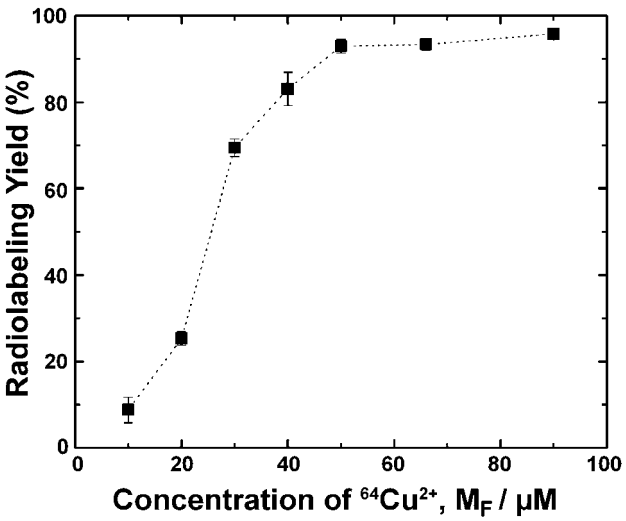

Fig. 7 Radiolabeling yield as a function of the final concentration of $^{64}Cu^{2+}$, M_F, using a 1 : 1 stoichiometric ratio of $^{64}Cu^{2+}$ to DOTA-*cyclo*(RGDfK). Error bars represent standard deviation in the extent of reaction for three experiments ($t_{RES} = 12$ minutes, $T = 37$ °C), using radiometal solutions made from the same batch of $^{64}Cu^{2+}$. Lines between points are guides for the eye.

performance of the microreactor by radiolabeling DOTA-*cyclo*(RGDfK) with $^{64}Cu^{2+}$. We show that the materials from which the microreactor is made can withstand substantial doses of radiation (260 mCi), and interact minimally with the radiometal, once the negatively charged glass surface of the microreactor is blocked with positively charged ions (~5% retention of injected activity). Furthermore, from a comparison between the radiolabeling yields of the microreactor and of two conventional radiolabeling methods at various temperatures, we conclude that the higher radiolabeling yield observed for the microreactor was achieved through efficient mixing with chaotic advection and through enhanced heat transfer. Finally, we demonstrate that, by using small volumes of concentrated radiometal (~50 µM), it is possible to achieve high radiolabeling yields (>90%) without resorting to using an excess of BFC–BM to accelerate the rate of reaction, as is necessary in macro-scale, conventional radiolabeling procedures that require dilution of the radiometal. High yields with a 1 : 1 stoichiometric ratio of radiometal to BFC–BM eliminate the need for chromatographic purification of the product to remove unlabeled BFC–BMs, resulting in shorter synthesis times and therefore a higher specific activity of the resulting imaging or therapeutic agent.

The results we report here suggest that this microreactor-based approach has potential for improving the preparation of radiopharmaceuticals in the clinic. We plan to further optimize chelation conditions for radiolabeling with other radiometals, such as ^{99m}Tc and ^{68}Ga, and to integrate pre-concentration and purification elements in the microreactor to ensure that high radiolabeling yields are obtained reproducibly, and that the radiometal solution is sufficiently pure and concentrated for the eventual clinical application of resulting radiopharmaceuticals in humans. Furthermore, we plan to develop a complementary microreactor for the conjugation of bifunctional chelators to disease-specific biomolecules. Such a system would provide great versatility for the production of patient-tailored doses of imaging and therapeutic agents for nuclear medicine.

Acknowledgements

We acknowledge financial support from the Department of Energy Office of Biological and Environmental Research, grant number DE-FG02-08ER64682. The production of $^{64}Cu^{2+}$ was supported by the National Institutes of Health, grant number R24 CA86307.

References

1 T. Leitha, *Curr. Pharm. Des.*, 2009, **15**, 173–187.
2 W. J. G. Oyen, L. Bodei, F. Giammarile, H. R. Maecke, J. Tennvall, M. Luster and B. Brans, *Ann. Oncol.*, 2007, **18**, 1782–1792.
3 S. Liu, *Adv. Drug Delivery Rev.*, 2008, **60**, 1347–1370.
4 C. J. Anderson and R. Ferdani, *Cancer Biother. Radiopharm.*, 2009, **24**, 379–393.
5 M. Shokeen and C. J. Anderson, *Acc. Chem. Res.*, 2009, **42**, 832–841.
6 S. V. Smith, *J. Inorg. Biochem.*, 2004, **98**, 1874–1901.
7 X. Chen, E. Sievers, Y. Hou, R. Park, M. Tohme, R. Bart, R. Bremner, J. R. Bading and P. S. Conti, *Neoplasia (Ann Arbor, MI, U. S.)*, 2005, **7**, 271–279.
8 J. S. Lewis, R. Laforest, T. L. Buettner, S.-K. Song, Y. Fujibayashi, J. M. Connett and M. J. Welch, *Proc. Natl. Acad. Sci. U. S. A.*, 2001, **98**, 1206–1211.
9 T. J. Wadas, E. H. Wong, G. R. Weisman and C. J. Anderson, *Curr. Pharm. Des.*, 2007, **13**, 3–16.
10 D. L. Kukis, S. J. DeNardo, G. L. DeNardo, R. T. O'Donnell and C. F. Meares, *J. Nucl. Med.*, 1998, **39**, 2105–2110.
11 T. J. Wadas and C. J. Anderson, *Nat. Protocols*, 2006, **1**, 3062–3068.
12 Y. Wu, X. Zhang, Z. Xiong, Z. Cheng, D. R. Fisher, S. Liu, S. S. Gambhir and X. Chen, *J. Nucl. Med.*, 2005, **46**, 1707–1718.
13 H. Audrain, *Angew. Chem., Int. Ed.*, 2007, **46**, 1772–1775.
14 A. M. Elizarov, *Lab Chip*, 2009, **9**, 1326–1333.
15 P. W. Miller, *J. Chem. Technol. Biotechnol.*, 2009, **84**, 309–315.
16 C.-C. Lee, G. Sui, A. Elizarov, C. J. Shu, Y.-S. Shin, A. N. Dooley, J. Huang, A. Daridon, P. Wyatt, D. Stout, H. C. Kolb, O. N. Witte, N. Satyamurthy, J. R. Heath, M. E. Phelps, S. R. Quake and H.-R. Tseng, *Science*, 2005, **310**, 1793–1796.
17 A. M. Elizarov, M. R. van Dam, Y. S. Shin, H. C. Kolb, H. C. Padgett, D. Stout, J. Shu, J. Huang, A. Daridon and J. R. Heat, *J. Nucl. Med.*, 2010, **51**, 282–287.
18 S. Y. Lu, P. Watts, F. T. Chin, J. Hong, J. L. Musachio, E. Briard and V. W. Pike, *Lab Chip*, 2004, **4**, 523–525.
19 A. D. Stroock, S. K. Dertinger, A. Ajdari, I. Mezic, H. A. Stone and G. M. Whitesides, *Science*, 2002, **295**, 647–651.
20 I. Dijkgraff and O. C. Boerman, *Cancer Biother. Radiopharm.*, 2009, **24**, 637–347.
21 G. Z. Ferl, R. A. Dumont, I. J. Hildebrandt, A. Armijo, R. Haubner, G. Reischl, H. Su, W. A. Weber and S.-C. Huang, *J. Nucl. Med.*, 2009, **50**, 250–258.
22 Z. Liu, Y. Yan, S. Liu, F. Wang and X. Chen, *Bioconjugate Chem.*, 2009, **20**, 1016–1025.
23 L. M. De Leon-Rodriguez and Z. Kovacs, *Bioconjugate Chem.*, 2008, **19**, 391–402.
24 Y. N. Xia and G. M. Whitesides, *Angew. Chem., Int. Ed.*, 1998, **37**, 551–575.
25 C. Huhn, R. Ramautar, M. Wuhrer and G. W. Somsen, *Anal. Bioanal. Chem.*, 2010, **396**, 297–314.

